

# Brightest group galaxies and the large-scale environment

H. E. Luparello<sup>1</sup>, M. Lares<sup>1</sup>, D. Paz<sup>1</sup>, C.Y. Yaryura<sup>1</sup>, D. G. Lambas<sup>1</sup> and N. Padilla<sup>2,3</sup>

<sup>1</sup>*Instituto de Astronomía Teórica y Experimental (CONICET-UNC). Observatorio Astronómico de Córdoba, Córdoba, Argentina*

<sup>2</sup>*Departamento de Astronomía y Astrofísica, Pontificia Universidad Católica de Chile, Santiago, Chile*

<sup>3</sup>*Centro de Astro-Ingeniería, Pontificia Universidad Católica de Chile, Santiago, Chile*

Released 2014 Xxxxx XX

## ABSTRACT

We study the dependence of the properties of group galaxies on the surrounding large-scale environment, using SDSS-DR7 data. Galaxies are ranked according to their luminosity within each group and classified morphologically by the Sérsic index. We have considered samples of the host groups in superstructures of galaxies, and elsewhere. We find a significant dependence of the properties of late-type brightest group galaxies on the large-scale environment: they show statistically significant higher luminosities and stellar masses, redder  $u-r$  colours, lower star formation activity and longer star-formation time-scale when embedded in superstructures. By contrast, the properties of the early-type brightest group galaxies are remarkably similar regardless of the group global environment. The other group member galaxies exhibit only the local influence of the group they inhabit. Our analysis comprises tests against the dependence on the host group luminosity and we argue that group brightest member properties are not only determined by the host halo, but also by the large-scale structure which can influence the accretion process onto their late-type brightest galaxies.

**Key words:** large-scale structure of the universe - statistics - data analysis

## 1 INTRODUCTION

The observed distribution of galaxies at large scales shows a complex network of filaments and voids (e.g. Joeveer et al. 1978; Zel-dovich et al. 1982; Einasto et al. 1996; Colless et al. 2001; Jaaniste et al. 2004; Einasto 2006; Abazajian et al. 2009). After extended galaxy surveys (York et al. 2000; Colless et al. 2001) were completed, this picture was widely studied and confirmed, and it is also supported by the analysis of several numerical simulations consistent with the standard cosmological model (Frisch et al. 1995; Bond et al. 1996; Sheth et al. 2003; Shandarin et al. 2004). The hierarchical structure formation model states that the distribution of matter evolves from small fluctuations in the early universe to form the complex observed large-scale configuration (see e.g. Press & Schechter 1974; Bardeen et al. 1986; White & Rees 1978). During this evolutionary gravitational process, galaxies initially flow from underdense to higher density regions (e.g. Gunn & Gott 1972). Thus, the formation of voids and superstructures can be considered as complementary processes retaining useful information to infer the cosmological parameters. The higher density regions, usually named superclusters, are preferentially located at the intersections of walls and filaments. The galaxy superclusters are the largest systems of the Universe, hosting a variety of galaxy systems such as groups and clusters of galaxies.

It is widely accepted that galaxy properties are strongly influenced by the local environment in which they reside (Blanton et al. 2003; Balogh et al. 2004; Kauffmann et al. 2004; Wilman et al. 2005; Baldry et al. 2006; Hou et al. 2009; Peng et al. 2010;

McGee et al. 2011; Patel et al. 2011; Sobral et al. 2011; Muzzin et al. 2012; Hou et al. 2013). However, recent studies have analysed the influence of large-scale structure over the systems that they host. It is well known that more luminous groups and clusters are located in higher density environments (Einasto et al. 2003, 2005; Croft et al. 2012; Yaryura et al. 2012; Luparello et al. 2013). Also, galaxy properties in these systems such as the star formation rate and colors depend on the large-scale structure (Binggeli 1982; Donoso et al. 2006; Einasto et al. 2007a; Crain et al. 2009; White et al. 2010). Lietzen et al. (2012) analyse galaxies in groups inhabiting different large-scale environments in the eighth data release (DR8) of the Sloan Digital Sky Survey (SDSS, York et al. 2000). They conclude that in high-density environments the amount of passive elliptical galaxies rises while the star-forming spirals decrease. Thus, considering equally rich groups, they contain a large fraction of elliptical galaxies when located in supercluster environments.

Within this framework, Einasto et al. (2014) confirm that local and global environments have a significant impact over the formation an evolution of galaxies. They also find that even supercluster morphologies influence galaxy properties. Using Minkowski functionals they characterize supercluster morphologies splitting them into spider and filament types. Filament-type superclusters contain a larger fraction of red, early and low star-forming galaxies than spider-type. Besides, red and star-forming galaxies hosted in spider-type superclusters present higher stellar masses than in filament-type. Moreover, equally rich groups located in filament-

type superclusters contain a large fraction of red, early-type galaxies, with large stellar masses and low star-formation rates.

Luparello et al. (2013) study differences between galaxy group properties according to the large-scale environment over the seventh data release (DR7) of the SDSS. They assert that the total galaxy density profile around groups is independent of the global environment. However, groups in superstructures have larger stellar mass content, higher velocity dispersions and older stellar populations than groups elsewhere. As they compare equal global luminosity groups, a proxy of the total mass, they conclude that groups in superstructures formed earlier than groups located in lower density regions. In the same line, Chon et al. (2014) provide evidence that the special environment of superclusters, as characterized by the X-ray luminosity function, originates from a top-heavy mass function.

The degree to which the large-scale structure of the universe determines properties of galaxies, irrespective of the local environment, is still a promising field to understand many aspects of galaxy formation and evolution. This subject has been recently addressed by a number of works, either on galaxy survey data (Tempel et al. 2011; Einasto et al. 2007b) or focusing on particular known superclusters, like Ursa Major (Krause et al. 2013), Coma (Cybulski et al. 2014), Shapley (Merluzzi et al. 2014) Sculptor and the Sloan Great Wall (Einasto et al. 2008). For example, Krause et al. (2013) analyse the distribution of galaxy groups in the Ursa Major Supercluster, finding that relaxed systems around high density peaks may have formed and evolved earlier than nonrelaxed systems, which are growing slower on the peripheries of lower density peaks. In another noteworthy study, Cybulski et al. (2014) explore the star-forming activity of galaxies located in different regions of the Coma Supercluster, concluding that the fraction of star-forming galaxies progressively decreases from voids to filaments. According to the authors, the fraction of blue galaxies declines as the environmental density rises.

Einasto et al. (2008) present a study of the Sculptor supercluster and the Sloan Great Wall, two of the richest superclusters in the 2dF Galaxy Redshift Survey. They find differences in the galaxy content according to the local density within the supercluster, with a smaller fraction of early-type galaxies towards the outskirts. A related study carried out on the 2dF redshift survey (Einasto et al. 2007b) shows evidence of a larger fraction of early-type galaxies in superclusters with a larger global density.

Tempel et al. (2011) state that the luminosity function of elliptical galaxies strongly depends on the environment, while the luminosity distributions of late-type galaxies are similar. More recently, The Shapley Supercluster Survey (ShaSS, Merluzzi et al. 2014) which covers a region of  $260 \text{ Mpc}^3$ , including the Shapley supercluster core and mapping nine Abell clusters and two poor clusters, searches for the role of cluster-scale mass assembly on galaxy evolution and possible connections between the properties of the cosmic structures.

In this paper we analyse different properties of galaxies in groups in order to assess their dependence on the surrounding large-scale structure. We have studied the correlation of galaxy properties, namely: luminosities, colours, star-formation rates, concentration index and time-scales, and the large-scale environment constraining the local environment through the selection of galaxy groups. This paper is organized as follows. In Section 2 we describe the data samples of galaxies, galaxy groups, and superstructures. We also describe in this section the use of Sérsic index to discriminate galaxy morphologies and the ranking of galaxy luminosities within each group. In Section 3 we analyse the prop-

erties of the brightest group galaxies and in Section 4 we address their dependence on large-scale environment. We summarize the results and state the main conclusions in Section 5. Throughout this paper, we adopt a concordance cosmological model ( $\Omega_\Lambda = 0.75$ ,  $\Omega_{\text{matter}} = 0.25$ ).

## 2 DATA AND SAMPLES

### 2.1 SDSS-DR7 Galaxy Catalogue

In the present work we use the Seventh Data Release (DR7, Abazajian et al. 2009) of the Sloan Digital Sky Survey (York et al. 2000), which is publicly available<sup>1</sup>. The footprint area comprised by the spectroscopic galaxy catalogue is 9380 sq.deg and its limiting apparent magnitude in the r-band is 17.77 (Strauss et al. 2002). We use a more conservative limit of 17.5 to ensure completeness in our samples, and in order to avoid saturation effects in the photometric pipeline, we consider galaxies fainter than  $r = 14.5$ <sup>2</sup>. We also use the value added galaxy catalog from MPA-JHU DR7 (Kauffmann et al. 2003), which provides additional information about star-formation rates and stellar masses. The star-formation rates (SFRs) are computed following the procedure described by Brinchmann et al. (2004), while the stellar masses are obtained as explained in Kauffmann et al. (2003) and Salim et al. (2007).

The one-component Sérsic fits to galaxy radial profiles can be used to roughly estimate the morphological galaxy classification (Blanton et al. 2003). We use Sérsic indices from the NYU Value-Added Galaxy Catalog (NYU-VAGC, Blanton et al. 2005) to separate two samples of galaxies with different morphological properties. Details about the chosen threshold values of the Sérsic indices and the properties of the subsamples are given in subsection 2.6.

### 2.2 SDSS-DR7 Superstructures

Galaxies in the universe are arranged in a supercluster-void network. Superclusters enclose a wide range of galaxy structures ranging from single galaxies to rich clusters. Thus, these environments may provide important clues to unveil galaxy formation physics, evolution and large-scale clustering.

There are several supercluster catalogues (e.g., Einasto et al. 2007; Costa-Duarte et al. 2011; Luparello et al. 2011; Liivamägi et al. 2012) constructed using the so called density field method. However, as these systems are going through their virialization process, there is a certain degree of freedom in defining the applied density threshold. According to the  $\Lambda$ CDM Concordance Cosmological Model, the present and future dynamics of the universe are dominated by an accelerated expansion. By combining the luminosity density field method (Einasto et al. 2007) with the theoretical criteria for the mass density threshold of Dünner et al. (2006), Luparello et al. (2011) presented a catalogue of so called Future Virialized Structures (FVS). The density field method allows to compute the galaxy luminosity density field by convolving the spatial distribution of galaxies with a kernel function weighted to the galaxy luminosity. We used an Epanechnikov kernel of  $8 \text{ h}^{-1} \text{ Mpc}$  to sample the density field into a redshift-space grid composed by cubes of  $1 \text{ h}^{-1} \text{ Mpc}$  side. We then select the highest luminosity density groups of cells to isolate the large structures. However, the exact value of the luminosity density threshold has been a matter of some

<sup>1</sup> <http://www.sdss.org/dr7>

<sup>2</sup> [http://www.sdss.org/dr7/products/general/target\\_quality.html](http://www.sdss.org/dr7/products/general/target_quality.html)

debate, since different values give rise to entirely different samples of superstructures. In a previous work (Luparello et al. 2011), we used a criterion motivated by dynamical considerations to calibrate this value. The resulting large-scale structures correspond to overdense regions in the present-day universe that will become virialized structures in the future. The catalogue of FVS was compiled using a volume-limited sample of galaxies from the SDSS-DR7, in the redshift range  $0.04 < z < 0.12$ , with a limiting absolute magnitude of  $M_r < -20.47$ . According to calibrations made using mock catalogues, the final sample of FVS is 90 per cent complete and has contamination below 5 per cent. The volume covered by the catalogue is  $3.17 \times 10^7 (h^{-1} \text{ Mpc})^3$ , within which 150 superstructures were identified, composed by a total of 11394 galaxies. FVS luminosities vary between  $10^{12} L_\odot$  and  $\approx 10^{14} L_\odot$ , and their volumes range between  $10^2 (h^{-1} \text{ Mpc})^3$  and  $10^5 (h^{-1} \text{ Mpc})^3$ .

### 2.3 SDSS-DR7 Group Catalogue

The clustering properties and the formation and evolution processes of mass in the scale of galaxy groups are a result of the hierarchical accretion of mass that also gives rise to luminous galaxies. For that reason, galaxy groups are key to observationally constrain those processes. To characterize the local environment of galaxies we use galaxy groups identified by Zapata et al. (2009) in the SDSS galaxy catalogue, extended to cover the SDSS-DR7. The identification method is based on a "Friends of Friends" algorithm, which is one of the most commonly used percolation algorithms. It allows to tie in sets of galaxies, where each galaxy is closer than a given linking length to at least another galaxy in the group. The parameters in the algorithm can be adjusted so that the resulting groups resemble the regions occupied by dark matter haloes. Following Merchan & Zandivarez (2005), Zapata et al. (2009) used a variable projected linking length and a fixed radial linking length, in order to compensate the decrease of the number of galaxies with redshift in flux-limited samples. The parameters of the percolation algorithm have been calibrated using mock catalogues, so that an optimal compromise between completeness and contamination is achieved. The varying projected linking length  $\sigma = \sigma_0 \times R$  has a value of  $\sigma_0 = 0.239 h^{-1} \text{ Mpc}$  (where  $R$  is the scaling factor as defined in equation (4) of Merchan & Zandivarez (2005)), and the fixed radial linking length is  $\Delta v = 450 \text{ km s}^{-1}$ . The configuration adopted for the FoF identification of galaxy groups corresponds to the values calibrated by Merchan & Zandivarez (2005) to obtain 95 per cent of completeness and 8 per cent of contamination. The identification is performed on a flux limited galaxy sample. The catalogue contains 83784 groups with at least 4 members, and is limited to redshift  $z < 0.2$ .

### 2.4 SDSS-DR7 Galaxy and Group samples

With the aim to study the impact of large-scale environment over galaxy properties, we analyse the variation of characteristic parameters of galaxies in groups inside and outside superstructures. First we select galaxy groups within the volume of the FVS catalogue with multiplicities between 5 and 15 members. We use a lower multiplicity limit of five members to diminish contamination and an upper limit of fifteen members taking into account Figure 2 of Luparello et al. (2013), who find that for  $n > 15$  the relation between multiplicity and group luminosity differs significantly between groups within FVS and elsewhere.

In addition, we compute total group luminosities using the

volume-limited sample of galaxies in groups within the limiting redshift. The limiting absolute magnitude in the r-band corresponding to the limiting redshift  $z = 0.12$  is  $M_{r\text{lim}} = -20.47$ . The total group luminosities (which can be considered as a proxy of group mass) were obtained by adding the r-band luminosities of the member galaxies brighter than  $M_{r\text{lim}}$ .

FVS are globally overdense systems, but they also have complex morphologies and their different regions present a wide range of density levels. To ensure that we are analyzing reliable samples, we select groups located in the densest cores of superstructures and not around their peripheral zones. In order to accomplish this, we estimate the mean luminosity density on a  $13 h^{-1} \text{ Mpc}$  side cube (which corresponds approximately to the volume of a sphere of radius  $8 h^{-1} \text{ Mpc}$ ) centered on each group. We keep groups with mean luminosity density equal or greater than 5.3 times the mean overall luminosity density estimated on the SDSS-DR7,  $\bar{\rho} = 1.73 \times 10^8 L_\odot$ . This threshold was chosen according to the calibration previously presented by Luparello et al. (2011). In order to have a suitable number of groups per luminosity bin, we also restrict group luminosities to the range  $10^{10.9} - 10^{11.35} L_\odot$ . Under these conditions, we obtain a sample of 123 groups inhabiting the densest regions of FVS. For an adequate comparison, we also select groups not belonging to FVS. By applying the same restrictions over group members and luminosities, we obtain a sample of 372 groups outside FVS. Regarding the galaxies that conform the group samples, we remove those with magnitude uncertainties greater than 0.05 in the r-band. The final samples comprise 861 galaxies in groups located in FVS and 2620 galaxies in groups out of FVS, in the redshift range  $0.04 \leq z \leq 0.12$ .

### 2.5 Luminosity gap in groups

We define the "luminosity ranking" of galaxies with respect to their host group, arranging them in descending order of r-band luminosity, then the brightest group galaxy (BGG) is the first ranked. The BGG properties and their relation with the environment have been widely studied. De Lucia et al. (2012) use galaxy merger trees from semi-analytic model simulated catalogues to study the histories of galaxies in groups according to their environment. In a hierarchical structure formation driven picture of the assembly of groups, the authors claimed that there is a history bias that shapes the properties of central and satellite galaxies and that to some extent depends on the large-scale structure. Shen et al. (2014) establish that BGGs are more luminous than expected from the ordered statistics, indicating that its distinctive brightness may be a consequence of physical processes rather than just an artifact of them being defined as the brightest galaxy in its group. They state that this brightening process, produced by the growth of stellar mass, may be associated to local processes.

When the gap in luminosity between the BGG and the rest of the members in the group is large, the system can be considered as a dominant galaxy with satellites. This type of systems has been studied to assess the role of the primary galaxy on the evolution of the group. By analysing the properties of faint satellites associated to isolated bright galaxies, Lares et al. (2011) conclude that the satellite overdensity depends on the luminosity and color of the primary galaxy and on the luminosity of the satellites. These systems of satellites around bright isolated galaxies are found to be more concentrated and more populated for red, passive galaxies, and for larger stellar mass central galaxies (Agustsson & Brainerd 2010; Guo et al. 2011; Lares et al. 2011; Wang & White 2012; Wang et al. 2014). Given this correlation, early-type brightest group galaxies

are expected to reside in more dynamically relaxed groups compared to those where the BGG is of late-type.

## 2.6 Group samples and galaxy classification

As stated above, BGG properties are strongly related to the intrinsic properties of their host groups. Taking this into account, we use the BGG characteristics to distinguish between different host group classes. Morphological classifications of galaxies have been linked to their formation and evolution (Pannella et al. 2009), as well as to their star formation and central black hole activity (Schawinski et al. 2010). Also, galaxy morphological types depend on the surrounding environment (Bamford et al. 2009).

The radial dependence of surface brightness of galaxies can be considered as an indicator of their morphology (Trujillo et al. 2001). The one-component Sérsic fits (Sérsic 1963; Sérsic 1968) to galaxy radial profiles can be used to roughly estimate the morphological galaxy classification (Blanton et al. 2003). The Sérsic profile,

$$I(r) = I_0 \exp[-(r/r_0)^{1/n}], \quad (1)$$

is parameterized by  $I_0$ , the central surface-brightness,  $r_0$ , the scale radius, and  $n$ , the profile index for each galaxy. The Sérsic index  $n$  is correlated to the morphological type:  $n = 4$  represents the profile of elliptical galaxies  $r^{1/4}$  (de Vaucouleurs 1948) while  $n = 1$  corresponds to the exponential profile of spiral disk galaxies. There are previous studies based on SDSS which consider the Sérsic index as a morphological indicator. Even though most of these studies assume empirical cutoffs around  $n = 2.5$  to establish morphological distinction, this value depends on the specific aim of the analysis. For instance, Blanton et al. (2003) divide the SDSS galaxies into two groups according to this index. They distinguish an exponential group with  $n < 1.5$  and a concentrated group with  $n > 3$ , analysing the relationships between galaxy parameters. Furthermore, Shen et al. (2003) choose  $n = 2.5$  which is the average between exponential and the Vaucouleurs profiles, while Hogg et al. (2003) apply  $n = 2$ .

In Figure 1(a), we show the Sérsic profile index  $n$  distributions for the galaxy samples inside (solid line) and outside (dashed line) FVS. We can notice that  $n$  presents a similar behavior in all galaxies, independently of the environment they are embedded in. However, as previously mentioned, this parameter allows us to make a morphological distinction between early and late-type galaxies according to their surface brightness profiles. In Figure 1(b) we show the Sérsic index distribution for the BGGs, inside (solid line) and outside (dashed line) FVS. It can be seen that the distributions do not depart significantly from each other, neither in the full sample nor the subsample of BGGs. According to these distributions, and for the sake of obtaining two samples of roughly the same size, we separate both galaxy samples by a threshold of  $n = 3.5$ , indicated by the dotted vertical line in panels (a) and (b). This is not the conventional value adopted to discriminate morphological characteristics of galaxies. Nevertheless, as our purpose is to study the brightest galaxy of each group, which tends to be red, early and elliptical, we employ a less restrictive value. This allows us to distinguish between a sample dominated by groups with an early-type brightest galaxy ( $n > 3.5$ ), and another sample dominated by groups with a late-type brightest galaxy ( $n < 3.5$ ). In an attempt to verify if this is a suitable classification, we visually inspect the brightest group galaxies of each sample, confirming that most of the brightest group galaxies with  $n > 3.5$  can be classified as early-type galaxies whereas those with  $n < 3.5$  are likely to be late-type galaxies. Using this criteria, we obtain four samples of galaxies in groups

within FVS	$E_{in}$	$L_{in}$	$Total_{in}$
$N_{grps}$	92	31	123
$N_{glxs}$	457	404	861
outside FVS	$E_{out}$	$L_{out}$	$Total_{out}$
$N_{grps}$	270	102	372
$N_{glxs}$	1382	1238	2620

**Table 1.** Size of galaxy samples in groups dominated by an early-type BGG ( $E_{in/out}$ ) or a late-type BGG ( $L_{in/out}$ ) inside and outside FVS, respectively.

described in Table 1. Sample  $E_{in}$  is composed by galaxies in groups dominated by an early-type galaxy and within a FVS; and sample  $E_{out}$  is composed by galaxies in groups dominated by an early-type galaxy not within a FVS environment. On the other hand, sample  $L_{in}$  comprises the galaxies in groups dominated by a late-type galaxy which also belong to a FVS and sample  $L_{out}$  contains the galaxies in groups outside FVS, dominated by a late-type galaxy.

We have also computed the luminosity gap mentioned in Section 2.5, ie. the luminosity difference between the first and second ranked galaxies in the groups, taking into account their morphologies and pertinence to FVS. In the lower panels of Figure 1, we show separately the luminosity gap for groups with a late-type BGG (c) and for groups with an early-type BGG (d), in FVS and elsewhere. The median of the luminosity gap for groups dominated by late-type galaxies is approximately -0.36, and is remarkably similar for groups in FVS and elsewhere. For early types this luminosity gap median is -0.40 for groups in FVS and -0.30 elsewhere, a small difference at the  $2\sigma$  level. Taking into account these results, the groups analysed can not be considered as extremely dominant galaxies with satellites.

## 2.7 Luminosity and multiplicity of group samples

Among group properties, the total group luminosity is one of the most relevant quantities, since it strongly correlates with group total mass and therefore with galaxy member properties. Lacerna et al. (2014) study the properties of halo-central galaxies and compare central galaxies in groups (host halos containing satellites) to isolated central galaxies (host halos without satellites). They find that group central galaxies are redder and less star forming than field central galaxies, although the color and specific star formation rate distributions at the same stellar mass are comparable. The authors argue that central galaxies which assembled in dense environments like groups or clusters, tend to have larger masses. Figure 2 shows the luminosity distribution for groups inside (solid line) and outside (dashed line) FVS. Vertical lines (solid line for galaxies inside FVS and dashed line for galaxies elsewhere) indicate the sample means, and the boxes represent the error estimated by standard deviation. The total group luminosity distribution is shown in the upper panel, and those corresponding to samples  $L_{in/out}$  and  $E_{in/out}$  in the lower panels, exhibiting that groups in FVS are more luminous than groups elsewhere. This enforces the fact that, in order to compare galaxies within and outside FVS, we have to take into account whether the properties of the group samples in FVS and elsewhere are similar. Firstly, we have checked that the distance distribution of group within FVS and elsewhere are similar, assuring no redshift dependent systematic effects. Besides, groups in samples  $L_{in}$  and  $L_{out}$  do not show significant luminosity differences respect to those between  $E_{in}$  and  $E_{out}$  samples. Moreover, the multiplicity could

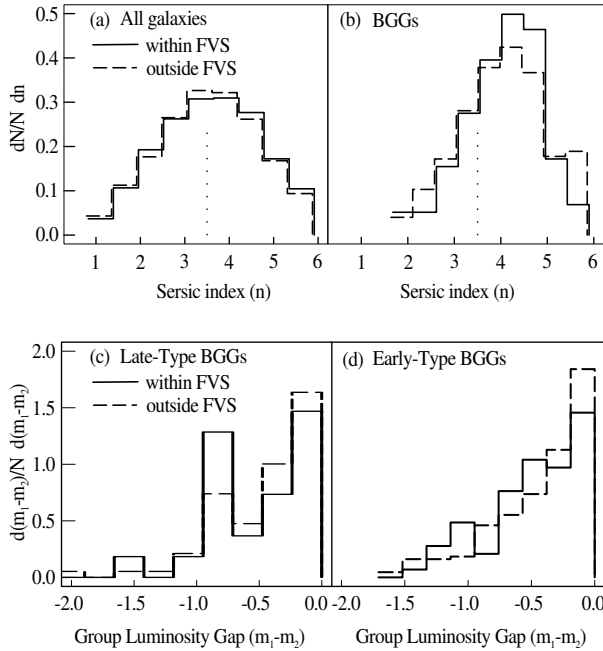


**Figure 1.** (a) Sérsic profile index ( $n$ ) histograms for galaxies within FVS (solid lines) and outside FVS (dashed lines). The same is shown in (b) for the sample of the brightest group galaxies. Dotted line in both panels indicates the threshold  $n = 3.5$ .

(c) Luminosity gap ( $m_1 - m_2$ ) histograms for groups with a late-type BGG within FVS (solid lines) and outside FVS (dashed lines). The same is shown in (d) for the groups with an early-type BGG.

have a significant effect on the comparison of galaxy groups. In the Figure 3 we show the mean group multiplicity  $N$  per bin of group luminosity, inside and outside FVS, comparing samples  $E_{in}$  (solid line) with  $E_{out}$  (dashed line) in the upper panel and  $L_{in}$  (solid line) with  $L_{out}$  (dashed line) in the lower panel. Bins of group luminosity are taken on an equal-number basis. As can be seen, in both cases the multiplicity has a similar behavior therefore we do not expect any systematic effect on the group comparison, except maybe on the highest luminosity groups dominated by late-type BGGs.

In figure 4 we show the luminosity density of the FVS associated to the Sloan Great Wall. The member groups are superimposed showing separately those dominated by early and late-type galaxies. The plot shows a similar distribution although with a tendency of groups dominated by late-type galaxies to lie in the outskirts. In the top of the figure it is shown the distribution of local densities in 13 Mpc cubic cells centered in each group of the total sample, where it can be seen that high density groups correspond approximately to those in FVS although there is a small fraction of groups with local high densities that are not member of FVS. With the use of FVS in our study, we are able to distinguish these regions of high global densities but that do not belong to superstructures.

### 3 PROPERTIES OF GROUP GALAXIES

In order to study the possible environmental effects on galaxies in groups, we analyse variations of properties associated to the star-formation activity, depending on whether they reside or not in FVS. For this aim, we have used the  $u - r$  color index that provides a

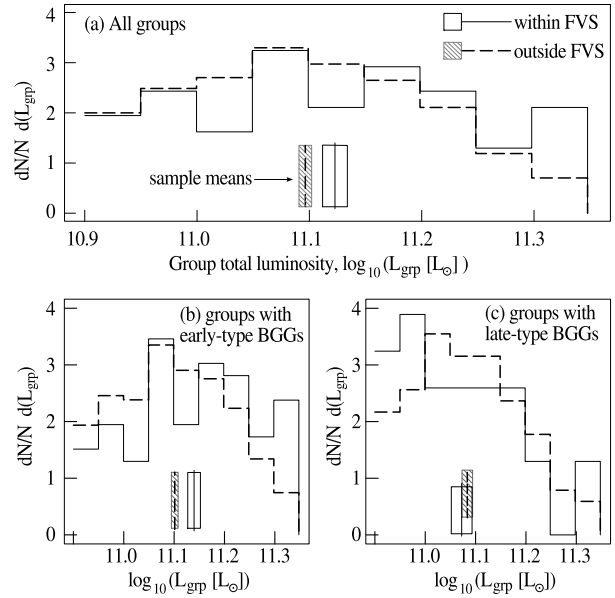


**Figure 2.**  $M_r$ -band total luminosity histograms of groups within FVS (solid lines) and outside FVS (dashed lines), for (a) the total sample of groups, (b) groups with an early-type brightest galaxy ( $E_{in/out}$  samples), and (c) groups with a late-type brightest galaxy ( $L_{in/out}$  samples). The means and mean uncertainties of the distributions are indicated by white and shaded boxes, for the samples of groups within and outside FVS, respectively.

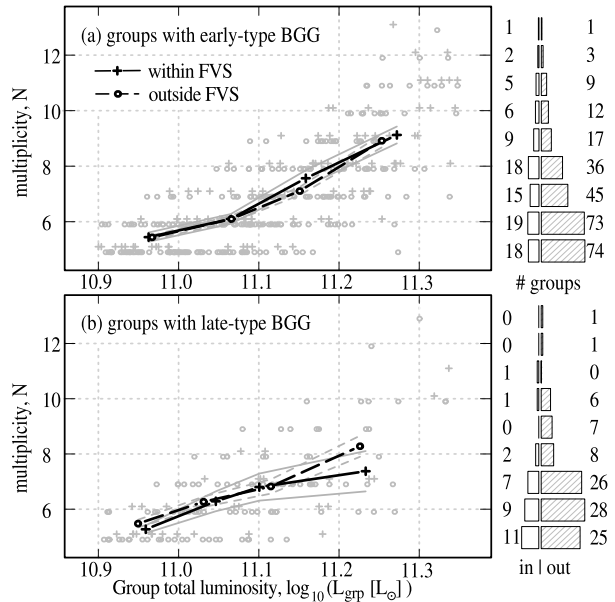


**Figure 3.** Mean multiplicity of groups within (solid lines) and outside (dashed lines) FVS, as a function of total group  $M_r$ -band luminosity, separately for (a, upper panel) groups with an early-type brightest galaxy, and (b, bottom panel) groups with a late-type brightest galaxy. The individual values of total group luminosity and multiplicity are represented for each group with grey cross symbols and circles, for groups within and outside FVS, respectively. Bar charts with the number of groups within (left bars) and outside (right, shaded bars) FVS per multiplicity value are shown on the right.

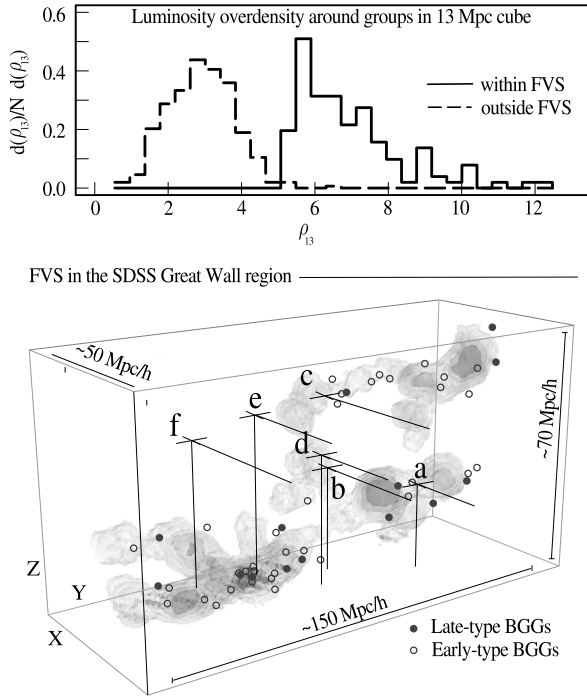


**Figure 4.** Top panel: distribution of local densities in 13 Mpc cubic cells centered in each group of the total sample. Solid line corresponds to groups in FVS and dashed line to groups elsewhere. Bottom panel: luminosity density of the FVS associated to the Sloan Great Wall. The positions are shown in a cartesian system associated to the equatorial coordinate system. Lighter shades of grey correspond to higher densities, and white corresponds to regions outside the Great Wall. The member groups are superimposed showing separately those dominated by early and late type galaxies. The crosses mark the centre of mass of the superclusters identified by Liivamägi et al. (2012) in the same region: (a) SCL 184+003+0077; (b) SCL 202-001+0084; (c) SCL 187+008+0089; (d) SCL 189+003+0086; (e) SCL 196+011+0086; (f) SCL 198+007+0093.

suitable indication of recent episodes of star formation. In spite of their larger uncertainties, we have used the  $u-r$  color index instead of  $g-r$  since we have shown in Lambas et al. (2012) that star formation induction can be successfully detected using this index.

In addition, we have also analysed the stellar mass content and star formation rate provided in the SDSS database. The concentration parameter  $R_{50}/R_{90}$  also provides a suitable measure of the light concentration.

### 3.1 Properties according to the galaxy ranking

We have studied the behaviour of mean  $u-r$  colors and stellar masses of the different samples as a function of galaxy ranking. In Figure 5 we show the mean  $u-r$  colors of samples  $E_{in}$  (solid line) and  $E_{out}$  (dashed line) in the top panel, and of samples  $L_{in}$  (solid line) and  $L_{out}$  (dashed line) in the bottom panel. All groups contribute with one galaxy up to ranking 5, but for higher ranking the averaged values are computed using only the richer groups. The vertical dashed lines in the Figure 5 indicate the completeness of the group samples. The environmental influence over galaxies in groups dominated by a late-type BGG is noticeable on the two more luminous galaxies (lower panel of Figure 5), which are redder if they belong to a group within FVS, with  $1-\sigma$  significance. Conversely, this effect is not noticeable for galaxies in groups dom-

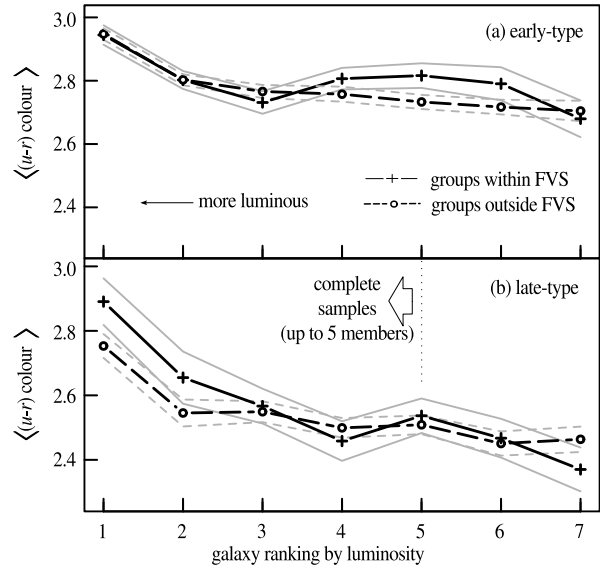


**Figure 5.** Mean  $u-r$  colors of (a) early-type and (b) late-type galaxies as a function of galaxy ranking, for groups within FVS (solid lines, cross symbols) and outside FVS (dashed lines, circles). Grey lines represent  $1-\sigma$  uncertainties.

inated by an early-type BGG. In the top panel of Figure 6 we show the variation of the mean stellar mass of samples  $E_{in}$  (solid line) and  $E_{out}$  (dashed line) as a function of galaxy ranking. Similarly, the results for samples  $L_{in}$  (solid line) and  $L_{out}$  (dashed line) are shown in the bottom panel of this Figure. In both panels it can be seen a similar trend, however there is a slight difference between samples  $L_{in}$  and  $L_{out}$ . This suggests that the environmental influence on stellar mass is just detectable for galaxies in groups dominated by a late-type BGG. By inspection of both figures, it can be seen that a significant effect appears in the first-ranked galaxy and decays for higher ranked galaxies. As analysed in subsection 2.5, it is interesting to notice that even though the luminosity gap in groups is not large, it is still the central galaxy the one that shows differences in its properties.

According to these results, hereafter we will explore in detail the effect of the FVS on the galaxy properties considering only the first-ranked galaxies (BGGs).

### 3.2 Brightest Group Galaxy and large-scale environment

To ensure that the features pointed out in the previous section are due to the influence of the the large-scale environment defined by FVS, we restrict the following analysis to bins with the same total group luminosity inside and outside FVS, characterizing the local environment of main galaxies by the luminosity of their host groups. According to the results of Section 3.1, galaxies other than the first-ranked do not show a large-scale environment dependence, thus in this section we study only the properties of the BGGs.

Besides the comparison on equal total luminosity groups, we aim at studying BGGs with similar morphology. Therefore, we analyse averaged properties of the BGGs as a function of the  $r$ -band total group luminosity, as shown in the different panels of Figure 7. In this Figure we show the  $r$ -band magnitude,  $u-r$  colour, star formation rate, stellar mass, nominal time-scale (the ratio of stellar mass to star formation rate) and concentration index, in the

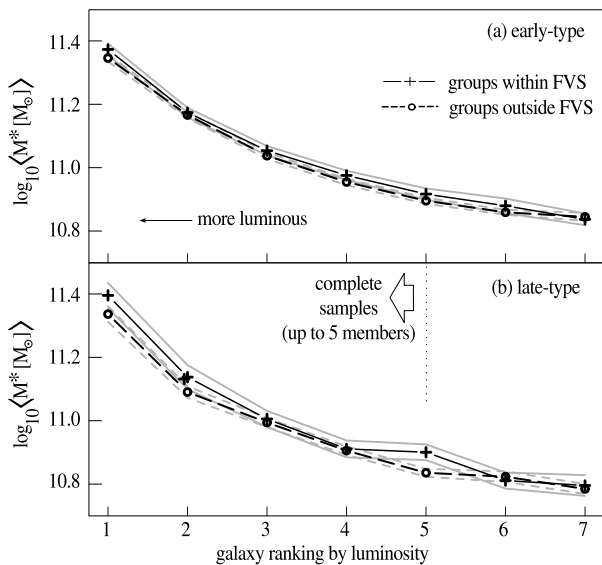


**Figure 6.** Mean stellar mass  $M^*$  of (a) early-type and (b) late-type galaxies as a function of galaxy ranking, for groups within FVS (solid lines, cross symbols) and outside FVS (dashed lines, circles). Grey lines represent  $1-\sigma$  uncertainties.

panels (a) to (f), respectively. In all cases, samples  $E_{in}$  and  $L_{in}$  are shown with solid lines, and samples  $E_{out}$  and  $L_{out}$  with dashed lines. Grey lines represent  $1-\sigma$  uncertainties of the averaged properties in each luminosity bin. In general, the difference between groups in high density peaks and groups not belonging to FVS is noticeable with a  $1-\sigma$  significance level, for the samples of groups with a late-type BGG ( $L_{in}$  and  $L_{out}$ ), over the entire group luminosity range (lower panel of Figure 7). This difference, however, is not significant for groups with an early-type BGG, as can be seen in the upper subpanels of the Figure 7.

Regarding to the  $M_r$  dependence on luminosity, it is clearly seen that the late-type BGGs in FVS are more luminous than their counterparts outside FVS (see Figure 7(a)). This trend is also evident from the marginal distributions (box plots at the right), where the medians of the early-type BGGs samples,  $E_{in}$  and  $E_{out}$ , are very similar, while late-type BGGs are noticeably more luminous when they are within FVS. The same trend can be noticed in the mean  $u-r$  colors, in Figure 7(b), where it can be seen that the late-type BGGs in FVS are redder than those outside FVS. Meanwhile, the early-type BGGs behave similarly regardless of their environment. With respect to the mean star formation rate (SFR) shown in Figure 7(c), there is also a tendency of the late-type BGGs to be less star-forming in FVS. Despite the more extended error bands, the difference in the mean SFR holds over the entire luminosity range (except may be for the less luminous groups) for late-type BGGs, but it is close to zero for the early-type BGG samples. For the less luminous groups, this effect inverts, showing a difference for the early-type BGGs, but not for the late-type. Figure 7(d) also shows that the mean stellar mass  $M^*$  for late-type BGGs is greater for galaxies in FVS than elsewhere. This difference also holds for groups in the whole luminosity range, and once again, is not significant for the early-type BGGs residing in groups of roughly the same total luminosity.

In order to assign an indicator of the galaxy time-scale we define the parameter  $\tau = M^*/SFR$ , which provides an estimate of the time-scale for the formation of the total stellar mass at the

present rate of star formation. This parameter is displayed in Figure 7(e) where, in spite of the errors, the late-type BGGs exhibit larger time-scales when they are in FVS. On the other hand, the concentration index correlates with galaxy morphological type (Shimasaku et al. 2001; Strateva et al. 2001; Nakamura et al. 2003) and is defined as the ratio of the two Petrosian radii  $C = R_{90}/R_{50}$  measured in the  $r$ -band, where  $R_{90}$  and  $R_{50}$  are radii corresponding to the apertures which include 90 per cent and 50 per cent of the Petrosian flux, respectively. In Figure 7(f) it can be seen that the early-type BGGs in FVS are slightly less concentrated than their counterparts outside FVS. For the late-type BGGs this effect is more remarkable and opposed; early-type galaxies are less concentrated if they lay within FVS, late-type BGGs are more concentrated when they belong to FVS. Finally, we have also explored samples of BGGs with equal luminosity distribution in FVS and elsewhere to check if the trends in color index, star-formation, age and concentration remain, or are due to the larger luminosities of BGGs in FVS. We find that the previously observed differences are similarly detected for these equal luminosity subsamples, reinforcing the astrophysical signals of the large-scale environment effect.

We acknowledge that contamination by background/foreground galaxies is likely to affect the total luminosities of a fraction of less than about 8 per cent of the groups (Zapata et al. 2009). However, we expect this contamination to be small given the relatively large number of true member galaxies and that this effect is expected to be uncorrelated with group properties. Besides, we argue that the previous results are not likely to be affected since our analysis relies on the brightest group members for which we expect a negligible contamination.

#### 4 QUANTIFYING THE LARGE-SCALE ENVIRONMENT DEPENDENCE OF EARLY AND LATE-TYPE BRIGHTEST GROUP GALAXIES

In order to quantify the large-scale environment dependence of early and late-type BGGs properties regardless the host group luminosity, we have considered departures from the mean values of such properties at a given group luminosity interval. For the complete sample of early (late) type BGGs, regardless of their location on the large-scale structure, we perform a linear fit of each property as a function of group luminosity. We then estimate the residuals of the fit, separately for the galaxies inside and outside FVS. If the FVS environment has no influence over galaxy properties, then these residuals should be distributed similarly. Otherwise, any trend on the mean of the residual values inside and outside FVS can be considered as an indicator of large-scale effects. This procedure resembles that of the principal component analysis, except that residuals in the axis measuring the galaxy property are used instead of the second principal component (Jolliffe 2005).

The mean residuals of the  $r$ -band absolute magnitude, the  $u-r$  color, the concentration index  $R_{50}/R_{90}$ , the logarithm of the star formation rate ( $\log_{10}(SFR)$ ), the stellar mass ( $\log_{10}(\text{stellar mass})$ ), and galaxy SFR time-scale ( $\log_{10}(\tau)$ ) are shown in Figure 8. Cross symbols and white boxes indicate BGGs inside FVS, and circles and grey boxes are used for BGGs outside FVS. The width of boxed regions around each symbol indicates the standard deviation. It can be seen that in most cases late-type BGGs exhibit more significant differences according to their large-scale environment while early-type BGGs are likely to belong to a common population, irrespective of whether they belong or not to a FVS. A remarkable exception to this uniformity in the early-type behaviour

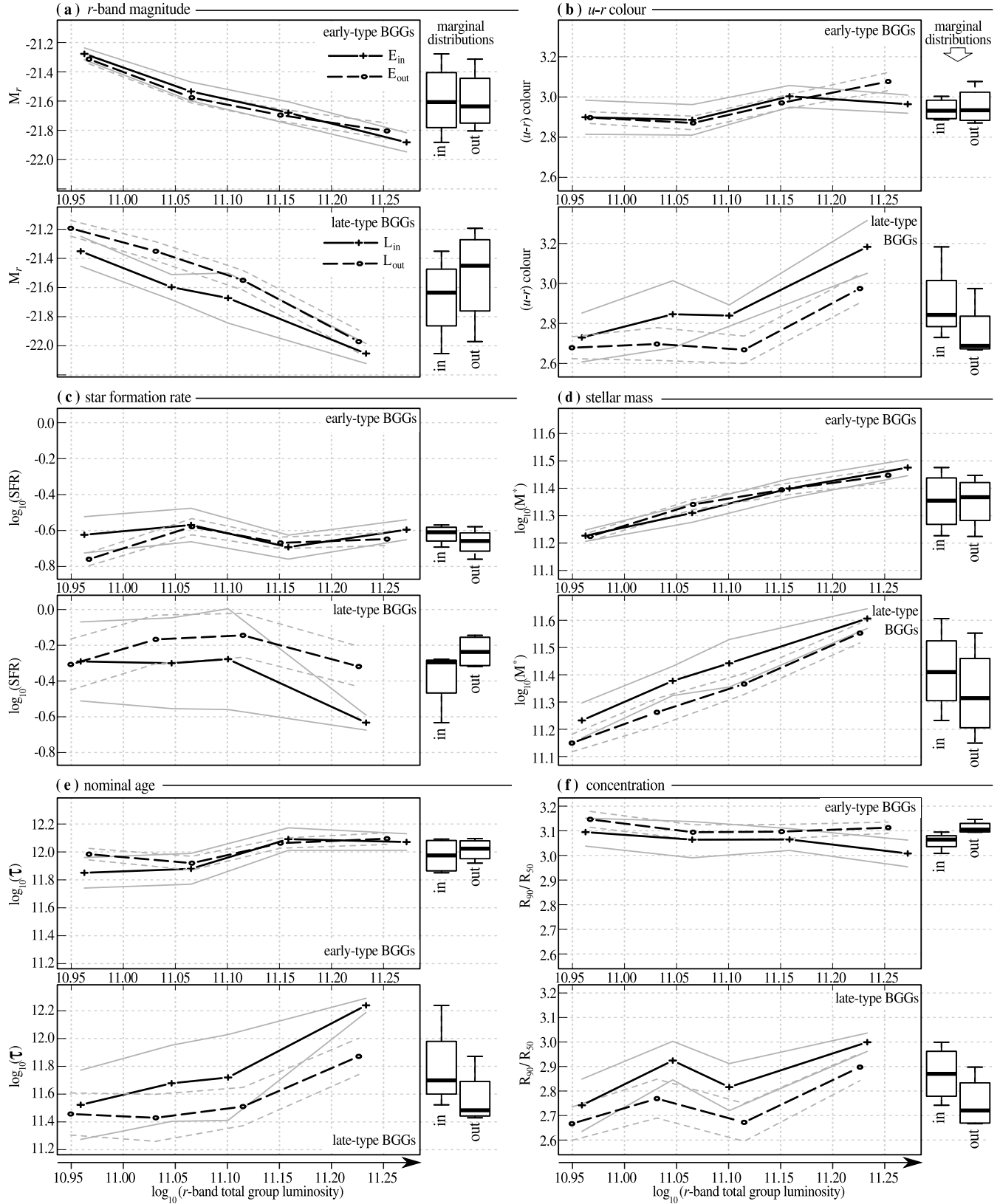


**Figure 7.** Averaged properties of early-type (upper subpanels) and late-type (lower subpanels) BGGs in FVS (solid lines) and elsewhere (dashed lines), as a function of total group luminosity.  $1-\sigma$  uncertainties are shown with solid and dashed gray lines, respectively. The properties shown in this Figure are a)  $r$ -band magnitude, b)  $u-r$  colour, c) star formation rate, d) stellar mass, e) nominal age and f) concentration index. In all panels  $L_{in}/L_{out}$  and  $E_{in}/E_{out}$  refer to late-type BGGs within/outside FVS and early-type BGGs within/outside FVS, respectively. Box plots on the right hand side of each panel show the quartiles and extrema of the corresponding marginal distributions.



is given by the concentration parameter, we recall this later below. First, let's consider the panel (a) of Figure 8. As it can be seen, early-type galaxies do not exhibit significant differences in the  $r$ -band magnitudes. For the late-type galaxies there are statistically significant differences indicating that BGGs outside FVS tend to be brighter than their corresponding sample in FVS. Secondly, in panel (b) of this figure, we find that late-type galaxies show noticeable differences in color residuals, depending on their FVS membership. Moreover late-type BGGs outside FVS have bluer residuals in comparison with systems inside FVS. However, it should be noticed that this difference is dominated by BGGs in FVS, since the mean of the residuals for this sample is  $0.11 \pm 0.06$  redder than the total mean, whereas the mean colour of BGGs outside FVS is not statistically different from the mean colour of the total sample. In contrast for early-type systems no dependency can be observed.

Following the analysis of Figure 8, in panel (c) we observe a marginally enhancement in the star formation rate for late-type systems outside FVS. We agree however that the obtained values lie inside the one standard deviation level significance. Even smaller differences are shown by early-type BGGs samples regardless of their FVS membership. Panel (d) shows a notable increment in stellar mass residuals for late-type BGGs inside superstructures. It should be noticed that residuals are computed over the logarithm of the mass, indicating that roughly a 10% of excess in stellar mass residuals for systems belonging to FVS respecting to galaxies outside superstructures. This signal goes in the same direction than the observed in panel (e) of Figure 8. In this panel we present the results for the logarithm of the star formation time-scale, depending on BGGs morphology and FVS membership. Here again we see an statistically significant difference for late-type systems whether they lay or not in FVS. Brightest late-type galaxies inside superstructures seem to be 30% older than its corresponding sample outside FVS. Finally, in panel (f) we show the results for residuals on the concentration parameter ( $R_{50}/R_{90}$ ). Remarkably, for this property we observe environment dependences for both galaxy morphologies. Early-type galaxies inside FVS exhibit notably less concentrated residuals than their analogous sample of field galaxies. This suggests that these systems may have been engaged in more frequently galaxy mergers than the field early-type galaxies. In contrast for late-type BGGs, we observe positive excess in concentration residuals in comparison to FVS member galaxies.

To quantify the statistical significance of these results, we consider a random set of subsamples of groups not belonging to FVS dominated by late-type galaxies and we compute the number of occurrences where the mean of the residuals of the different brightest galaxy properties is greater or equal than that corresponding to the dominant galaxy in FVS groups. We apply a resampling-method estimation using  $10^4$  random realizations of subsamples of groups not belonging to FVS finding that the difference between the sample averages of inner and outer late-type galaxies is statistically significant. The null hypothesis of the samples of late-type galaxies in and out FVS being part of the same parent distribution can be disproved up to a significance level of 90 per cent.

We confirm that late-type BGGs are brighter, redder, less star-forming, with a higher content of stellar mass, a larger time-scale for star formation, and more concentrated when they are inhabiting FVS than elsewhere. It is possible that these differences are due to the different large-scale amplitude of clustering of equal luminosity groups inside and outside FVS. However, we have tested different virial mass thresholds for group samples outside FVS to analyse whether their BGGs have properties comparable to the total group

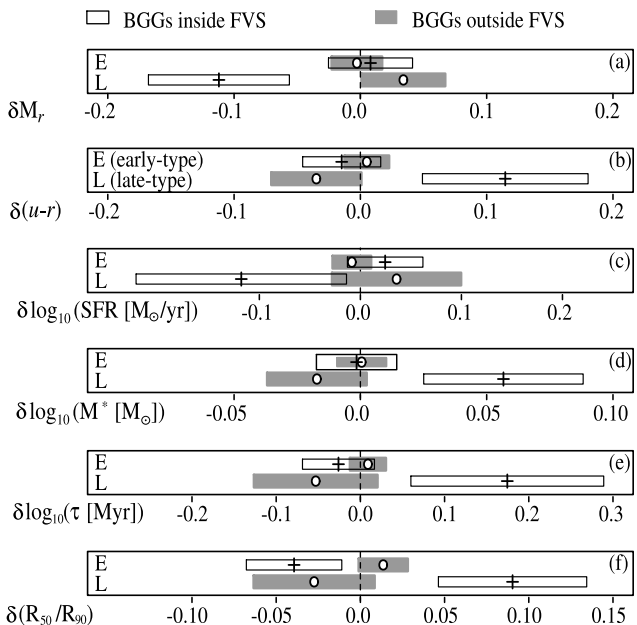


**Figure 8.** Mean residuals and their standard errors for early-type (E) and late-type (L) BGGs. The residuals are computed for (a)  $M_r$ -band luminosity, (b)  $u-r$  colour index, (c) star formation rate, (d) stellar mass, (e) nominal galaxy time-scale, and (f) concentration index. White boxes and cross symbols correspond to galaxies in groups within FVS ( $E_{in}$  and  $L_{in}$  samples), grey boxes and circles correspond to galaxies in groups outside FVS ( $E_{out}$  and  $L_{out}$  samples).

sample in FVS. We find that outside FVS, groups with masses as large as  $M_{vir} > 10^{14.4} M_{\odot}$  have to be considered so that their BGG properties are similar to the group sample in FVS. The relevance of the results shown in this section can be assessed by the fact that this high mass group subsample outside FVS roughly corresponds to the 10 per cent of more massive groups so that the large-scale environment does play a fundamental role in setting the properties of BGGs.

## 5 DISCUSSION AND CONCLUSIONS

As described in Section 1, there are several previous studies focused on the effects of the large-scale structure on galaxy properties (e.g., Binggeli 1982; Einasto et al. 2003, 2005; Donoso et al. 2006; Einasto et al. 2007a; Crain et al. 2009; White et al. 2010; Croft et al. 2012; Yaryura et al. 2012; Einasto et al. 2014, and references therein). Within this framework, our main concern is to investigate and quantify the large-scale dependence of the properties of galaxies in groups. To this end, we have analysed properties of galaxies that reside in similar local environments, by comparing samples in equal group total luminosity (mass) intervals. Our procedure has the advantage of separating the local and the global effects on group members.

The properties of the brightest group galaxy (BGG) and their host groups are strongly correlated (Agustsson & Brainerd 2010; Guo et al. 2011; Lares et al. 2011; Wang & White 2012; Wang et al. 2014). We can consider that early-type BGGs reside typically in more dynamically relaxed groups than those where the BGG is of late-type. Taking this into account, we characterized the BGGs according to their Sérsic index  $n$  (used as an estimator of morphology, see section 2.6 for details), and we defined four subsamples

of group galaxies:  $E_{in-out}$  dominated by an early-type BGG, and  $L_{in-out}$ , dominated by a late-type BGG, residing in superstructures or elsewhere, respectively. Besides, we have ordered the member galaxies according to their luminosity in order to assess the importance of the ranking within the groups in the response to the large-scale associated effects.

We can derive several conclusions from our study, concerning the influence of the structure at large scales on the properties of individual galaxies within groups, independently of the local environment given by the group properties. The main result is that the brightest galaxy within groups is by far more affected than the rest of group members. In fact, the change in the properties of galaxies beyond rank three in luminosity are negligible, although they exhibit the influence of the local environment given by the mass of the group they inhabit. The effects on the second brightest galaxy are marginally detected. The influence of the large scale on the BGGs does manifest on their colours, star formation rate, stellar mass content, concentration index and nominal age, and strongly depend on the galaxy type. While the properties of late-type BGGs differ significantly according to the large-scale structure, the averaged values of the properties of early-type galaxies are consistent within uncertainties. Late-type brightest group galaxies show statistically significant higher luminosities and stellar masses, redder  $u-r$  colours, lower star formation activity and larger star-formation time-scale when embedded in superstructures, and regardless of the group local environment. Our analysis comprises tests against the dependence on the host group luminosity, so that the effects of local environment, given by the properties of the group, and large-scale environment, given by the properties of the FVS, are disentangled. We argue that group brightest member properties are not only determined by the host halo, but also by the large-scale structure. Since the differences are significant only for late-type galaxies, they could be produced by the dependence of the accretion process onto the brightest galaxies, which in turn is conditioned by the mass overdensity at early times, and thus manifested today at large scales.

Previous works by different authors have analysed the correlation between group environment and the properties of their member galaxies. Lietzen et al. (2012) conclude that member galaxies in groups with similar richness are more likely to be passive if they are in superclusters. Einasto et al. (2014) find that supercluster morphology affects the galaxy population: filament-type superclusters contain a larger fraction of red, early and low star-forming galaxies than spider-type superclusters. Also, they find that blue, high SFR galaxies have lower environmental densities (defined within an  $8Mpc/h$  smoothing length) than red, low SFR galaxies in both types of superclusters. Einasto et al. (2011) study the role of the first ranked galaxies in groups in the region of the Sloan Great Wall finding that the spatial distribution of groups in the context of their hosting superclusters depend on whether they have an elliptical or spiral brightest galaxy. Luparello et al. (2013) compare equal global luminosity groups (a proxy of the total mass) concluding that groups in superstructures formed earlier than groups located in lower density regions. Consistently, we conclude that late-type BGGs inhabiting superstructures show 10 per cent higher luminosities, 10 per cent stellar mass excess, 0.11 redder  $u-r$  colours, significantly lower star formation activity and with a 30 per cent longer star-formation time-scales with respect to the means of the total samples (see section 4 for details of these calculations). These differences are negligible when considering lower luminosity galaxies, indicating that the effects are related to the particular role of the brightest group galaxy.

We argue that these differences are only found in late-type BGGs because of their formation history. The observed signals support a scenario where the gas accretion via mergers (relative to that of the stars) into the BGG is more important when the groups are located outside FVS. The accretion occurring in groups inhabiting FVS could be dominated by local dynamical processes such as galaxy harassment and gas extrangulation, resulting in a negligible effect of the FVS environment over low ranked galaxies. The more efficient accretion of gas onto the BGG not residing in FVS would be associated to the effects on late-type BGGs. Although this effect could also be present on early-type BGGs, their older ages could have erased the effect on these objects. However, the concentration parameter of early-type BGGs in FVS is significantly lower suggesting more recent merger events. In sum, our results indicate a significantly larger fraction of dry mergers compared to wet mergers, occurring onto BGGs in FVS.

## ACKNOWLEDGEMENTS

We thank the Referee, Maret Einasto, for her thorough review and highly appreciate the comments and suggestions, which greatly improved this work. This work was partially supported by the Consejo Nacional de Investigaciones Científicas y Técnicas (CONICET), and the Secretaría de Ciencia y Tecnología, Universidad Nacional de Córdoba, Argentina. NP was supported by Fondecyt regular 1110328 and BASAL CATA PFB-06. Funding for the SDSS and SDSS-II has been provided by the Alfred P. Sloan Foundation, the Participating Institutions, the National Science Foundation, the U.S. Department of Energy, the National Aeronautics and Space Administration, the Japanese Monbukagakusho, the Max Planck Society, and the Higher Education Funding Council for England. The SDSS Web Site is <http://www.sdss.org/>. The SDSS is managed by the Astrophysical Research Consortium for the Participating Institutions. The of the Royal Astronomical Society Participating Institutions are the American Museum of Natural History, Astrophysical Institute Potsdam, University of Basel, University of Cambridge, Case Western Reserve University, University of Chicago, Drexel University, Fermilab, the Institute for Advanced Study, the Japan Participation Group, Johns Hopkins University, the Joint Institute for Nuclear Astrophysics, the Kavli Institute for Particle Astrophysics and Cosmology, the Korean Scientist Group, the Chinese Academy of Sciences (LAMOST), Los Alamos National Laboratory, the Max-Planck-Institute for Astronomy (MPIA), the Max-Planck-Institute for Astrophysics (MPA), New Mexico State University, Ohio State University, University of Pittsburgh, University of Portsmouth, Princeton University, the United States Naval Observatory, and the University of Washington. Plots are made using R software and post-processed with Inkscape.

## REFERENCES

- Abazajian K. N., Adelman-McCarthy J. K., Agüeros M. A., Allam S. S., Allende Prieto C., An D., Anderson K. S. J., Anderson S. F., Annis J., Bahcall N. A., et al. 2009, *ApJS*, 182, 543
- Agustsson I., Brainerd T. G., 2010, *ApJ*, 709, 1321
- Baldry I. K., Balogh M. L., Bower R. G., Glazebrook K., Nichol R. C., Bamford S. P., Budavari T., 2006, *MNRAS*, 373, 469
- Balogh M. L., Baldry I. K., Nichol R., Miller C., Bower R., Glazebrook K., 2004, *ApJL*, 615, L101

- Bamford S. P., Nichol R. C., Baldry I. K., Land K., Lintott C. J., Schawinski K., Slosar A., Szalay A. S., Thomas D., Torki M., Andreescu D., Edmondson E. M., Miller C. J., Murray P., Rad-dick M. J., Vandenberg J., 2009, *MNRAS*, 393, 1324
- Bardeen J. M., Bond J. R., Kaiser N., Szalay A. S., 1986, *ApJ*, 304, 15
- Binggeli B., 1982, *A&A*, 107, 338
- Blanton M. R., Eisenstein D., Hogg D. W., Schlegel D. J., Brinkmann J., 2005, *ApJ*, 629, 143
- Blanton M. R., Hogg D. W., Bahcall N. A., Baldry I. K., Brinkmann J., Csabai I., Eisenstein D., et al. 2003, *ApJ*, 594, 186
- Bond J. R., Kofman L., Pogossyan D., 1996, *Nature*, 380, 603
- Brinchmann J., Charlot S., White S. D. M., Tremonti C., Kauffmann G., Heckman T., Brinkmann J., 2004, *MNRAS*, 351, 1151
- Chon G., Böhringer H., Collins C. A., Krause M., 2014, *A&A*, 567, A144
- Colless M., Dalton G., Maddox S., Sutherland W., Norberg P., Cole S., Bland-Hawthorn J., Bridges T., et al. 2001, *MNRAS*, 328, 1039
- Costa-Duarte M. V., Sodré Jr. L., Durret F., 2011, *MNRAS*, 411, 1716
- Crain R. A., Theuns T., Dalla Vecchia C., Eke V. R., Frenk C. S., Jenkins A., Kay S. T., Peacock J. A., Pearce F. R., Schaye J., Springel V., Thomas P. A., White S. D. M., Wiersma R. P. C., 2009, *MNRAS*, 399, 1773
- Croft R. A. C., Matteo T. D., Khandai N., Springel V., Jana A., Gardner J. P., 2012, *MNRAS*, 425, 2766
- Cybulski R., Yun M. S., Fazio G. G., Gutermuth R. A., 2014, *MNRAS*
- De Lucia G., Weinmann S., Poggianti B. M., Aragón-Salamanca A., Zaritsky D., 2012, *MNRAS*, 423, 1277
- de Vaucouleurs G., 1948, *Annales d'Astrophysique*, 11, 247
- Donoso E., O'Mill A., Lambas D. G., 2006, *MNRAS*, 369, 479
- Dünner R., Araya P. A., Meza A., Reisenegger A., 2006, *MNRAS*, 366, 803
- Einasto J., 2006, *Communications of the Konkoly Observatory Hungary*, 104, 163
- Einasto J., Einasto M., Tago E., Saar E., Hutsi G., Joeveer M., Liivamägi L., Suhhonenko I., Jaaniste J., Heinamäki P., Müller V., Knebe A., Tucker D., 2007, *A&A*, 462, 811
- Einasto J., Tago E., Einasto M., Saar E., Suhhonenko I., Heinamäki P., Hutsi G., Tucker D., 2005, *A&A*, 439, 45
- Einasto M., Einasto J., Müller V., Heinamäki P., Tucker D., 2003, *A&A*, 401, 851
- Einasto M., Einasto J., Tago E., Saar E., Liivamägi L. J., Joeveer M., Hutsi G., Heinamäki P., Müller V., Tucker D., 2007a, *A&A*, 464, 815
- Einasto M., Einasto J., Tago E., Saar E., Liivamägi L. J., Joeveer M., Hutsi G., Heinamäki P., Müller V., Tucker D., 2007b, *A&A*, 464, 815
- Einasto M., Lietzen H., Tempel E., Gramann M., Liivamägi L. J., Einasto J., 2014, *A&A*, 562, A87
- Einasto M., Liivamägi L. J., Tempel E., Saar E., Tago E., Einasto P., Enkvist I., Einasto J., Martínez V. J., Heinamäki P., Nurmi P., 2011, *ApJ*, 736, 51
- Einasto M., Saar E., Martínez V. J., Einasto J., Liivamägi L. J., Tago E., Starck J.-L., Müller V., Heinamäki P., Nurmi P., Paredes S., Gramann M., Hutsi G., 2008, *ApJ*, 685, 83
- Einasto M., Tago E., Jaaniste J., Einasto J., Andernach H., 1996, *VizieR Online Data Catalog*, 412, 30119
- Frisch P., Einasto J., Einasto M., Freudling W., Fricke K. J., Gramann M., Saar V., Toomet O., 1995, *A&A*, 296, 611
- Gunn J. E., Gott III J. R., 1972, *ApJ*, 176, 1
- Guo Q., Cole S., Eke V., Frenk C., 2011, *MNRAS*, 417, 370
- Hogg D. W., Blanton M. R., Eisenstein D. J., Gunn J. E., Schlegel D. J., Zehavi I., Bahcall N. A., Brinkmann J., Csabai I., Schneider D. P., Weinberg D. H., York D. G., 2003, *ApJL*, 585, L5
- Hou A., Parker L. C., Balogh M. L., McGee S. L., Wilman D. J., Connelly J. L., Harris W. E., Mok A., Mulchaey J. S., Bower R. G., Finoguenov A., 2013, *MNRAS*, 435, 1715
- Hou A., Parker L. C., Harris W. E., Wilman D. J., 2009, *ApJ*, 702, 1199
- Jaaniste J., Einasto M., Einasto J., 2004, *Ap&SS*, 290, 187
- Joeveer M., Einasto J., Tago E., 1978, *MNRAS*, 185, 357
- Jolliffe I., 2005, *Principal component analysis*. Wiley Online Library
- Kauffmann G., Heckman T. M., White S. D. M., Charlot S., Tremonti C., Brinchmann J., Bruzual G., et al. 2003, *MNRAS*, 341, 33
- Kauffmann G., White S. D. M., Heckman T. M., Ménard B., Brinchmann J., Charlot S., Tremonti C., Brinkmann J., 2004, *MNRAS*, 353, 713
- Krause M. O., Ribeiro A. L. B., Lopes P. A. A., 2013, *A&A*, 551, A143
- Lacerna I., Rodríguez-Puebla A., Avila-Reese V., Hernández-Toledo H. M., 2014, *ApJ*, 788, 29
- Lambas D. G., Alonso S., Mesa V., O'Mill A. L., 2012, *A&A*, 539, A45
- Lares M., Lambas D. G., Domínguez M. J., 2011, *AJ*, 142, 13
- Lietzen H., Tempel E., Heinamäki P., Nurmi P., Einasto M., Saar E., 2012, *A&A*, 545, A104
- Liivamägi L. J., Tempel E., Saar E., 2012, *A&A*, 539, A80
- Luparello H., Lares M., Lambas D. G., Padilla N., 2011, *MNRAS*, 415, 964
- Luparello H. E., Lares M., Yaryura C. Y., Paz D., Padilla N., Lambas D. G., 2013, *MNRAS*, 432, 1367
- McGee S. L., Balogh M. L., Wilman D. J., Bower R. G., Mulchaey J. S., Parker L. C., Oemler A., 2011, *MNRAS*, 413, 996
- Merchan M. E., Zandivarez A., 2005, *ApJ*, 630, 759
- Merluzzi P., Busarello G., Haines C. P., Mercurio A., Okabe N., Pimblett K. A., Dopita M. A., Grado A., Limatola L., Bourdin H., Mazzotta P., Capaccioli M., Napolitano N. R., Schipani P., 2014, *ArXiv Astrophysics e-prints*, astro-ph/1407.4628
- Muzzin A., Wilson G., Yee H. K. C., Gilbank D., Hoekstra H., Demarco R., Balogh M., van Dokkum P., Franx M., Ellingson E., Hicks A., Nantais J., Noble A., Lacy M., Lidman C., Rettura A., Surace J., Webb T., 2012, *ApJ*, 746, 188
- Nakamura O., Fukugita M., Yasuda N., Loveday J., Brinkmann J., Schneider D. P., Shimasaku K., SubbaRao M., 2003, *AJ*, 125, 1682
- Pannella M., Gabasch A., Goranova Y., Drory N., Hopp U., Noll S., Saglia R. P., Strazzullo V., Bender R., 2009, *ApJ*, 701, 787
- Patel S. G., Kelson D. D., Holden B. P., Franx M., Illingworth G. D., 2011, *ApJ*, 735, 53
- Peng Y.-j., Lilly S. J., Kovač K., Bolzonella M., Pozzetti L., Renzini A., Zamorani G., Ilbert O., Knobel C., Iovino A., Maier C., Cucciati O., 2010, *ApJ*, 721, 193
- Press W. H., Schechter P., 1974, *ApJ*, 187, 425
- Salim S., Rich R. M., Charlot S., Brinchmann J., Johnson B. D., Schiminovich D., Seibert M., Mallery R., Heckman T. M., Forster K., Friedman P. G., Martin D. C., Morrissey P., Neff S. G., Small T., 2007, *ApJS*, 173, 267
- Schawinski K., Urry C. M., Virani S., Coppi P., Bamford S. P.,

- Treister E., Lintott C. J., Sarzi M., Keel W. C., Kaviraj S., Cardamone C. N., 2010, *ApJ*, 711, 284
- Sérsic J. L., 1963, *Boletín de la Asociación Argentina de Astronomía La Plata Argentina*, 6, 41
- Sérsic J. L., 1968, *Atlas de galaxias australes*. Córdoba, Argentina: Observatorio Astronómico, 1968
- Shandarin S. F., Sheth J. V., Sahni V., 2004, *MNRAS*, 353, 162
- Shen S., Mo H. J., White S. D. M., Blanton M. R., Kauffmann G., Voges W., Brinkmann J., Csabai I., 2003, *MNRAS*, 343, 978
- Shen S., Yang X., Mo H., van den Bosch F., More S., 2014, *ApJ*, 782, 23
- Sheth J. V., Sahni V., Shandarin S. F., Sathyaprakash B. S., 2003, *MNRAS*, 343, 22
- Shimasaku K., Fukugita M., Doi M., Hamabe M., Ichikawa T., Okamura S., Sekiguchi M., Yasuda N., Brinkmann J., Csabai I., Ichikawa S.-I., Ivezić Z., Kunszt P. Z., Schneider D. P., Szokoly G. P., Watanabe M., York D. G., 2001, *AJ*, 122, 1238
- Sobral D., Best P. N., Smail I., Geach J. E., Cirasuolo M., Garn T., Dalton G. B., 2011, *MNRAS*, 411, 675
- Strateva I., Ivezić Ž., Knapp G. R., Narayanan V. K., Strauss M. A., Gunn J. E., Lupton R. H., Schlegel D., Bahcall N. A., et al. 2001, *AJ*, 122, 1861
- Strauss M. A., Weinberg D. H., Lupton R. H., Narayanan V. K., Annis J., Bernardi M., Blanton M., Burles S., Connolly A. J., Dalcanton J., Doi M., Eisenstein D., et al. 2002, *AJ*, 124, 1810
- Tempel E., Saar E., Liivamägi L. J., Tamm A., Einasto J., Einasto M., Müller V., 2011, *A&A*, 529, A53
- Trujillo I., Graham A. W., Caon N., 2001, *MNRAS*, 326, 869
- Wang W., Sales L. V., Henriques B. M. B., White S. D. M., 2014, *ArXiv Astrophysics e-prints*, astro-ph/1403.2409
- Wang W., White S. D. M., 2012, *MNRAS*, 424, 2574
- White M., Cohn J. D., Smit R., 2010, *MNRAS*, 408, 1818
- White S. D. M., Rees M. J., 1978, *MNRAS*, 183, 341
- Wilman D. J., Balogh M. L., Bower R. G., Mulchaey J. S., Oemler A., Carlberg R. G., Morris S. L., Whitaker R. J., 2005, *MNRAS*, 358, 71
- Yaryura C. Y., Lares M., Luparello H. E., Paz D. J., Lambas D. G., Padilla N., Sgró M. A., 2012, *MNRAS*, 426, 708
- York D. G., Adelman J., Anderson Jr. J. E., Yanny B., Yasuda N., 2000, *AJ*, 120, 1579
- Zapata T., Perez J., Padilla N., Tissera P., 2009, *MNRAS*, 394, 2229
- Zeldovich I. B., Einasto J., Shandarin S. F., 1982, *Nature*, 300, 407